HHS Public Access

Author manuscript

*Biofabrication*. Author manuscript; available in PMC 2021 April 22.

Published in final edited form as:

*Biofabrication*. ; 8(3): 035011. doi:10.1088/1758-5090/8/3/035011.

# Complex, multi-scale small intestinal topography replicated in cellular growth substrates fabricated via chemical vapor deposition of Parylene C

**Abigail N. Koppes**[1], **Megha Kamath**[2], **Courtney A. Pfluger**[1], **Daniel D. Burkey**[1,3], **Mehmet Dokmeci**[4,5,6], **Lin Wang**[1,7], **Rebecca L. Carrier**[1]

[1]Northeastern University, Chemical Engineering, Boston, Massachusetts, USA.

[2]Northeastern University, Pharmaceutical Sciences, Boston, Massachusetts, USA.

[3]University of Connecticut, Chemical and Biomolecular Engineering, Storrs, Connecticut, USA.

[4]Northeastern University, Electrical and Computer Engineering, Boston, Massachusetts, USA.

[5]Biomaterials Innovation Research Center, Division of Biomedical Engineering, Department of Medicine, Brigham and Women's Hospital, Harvard Medical School, Cambridge, Massachusetts, USA.

[6]Harvard-MIT Division of Health Sciences and Technology, Massachusetts Institute of Technology, Cambridge, Massachusetts, USA.

[7]GE Global Research-Shanghai, China.

## Abstract

Native small intestine possesses distinct multi-scale structures (e.g., crypts, villi) not included in traditional 2D intestinal culture models for drug delivery and regenerative medicine. The known impact of structure on cell function motivates exploration of the influence of intestinal topography on the phenotype of cultured epithelial cells, but the irregular, macro- to submicron-scale features of native intestine are challenging to precisely replicate in cellular growth substrates. Herein, we utilized chemical vapor deposition (CVD) of Parylene C on decellularized porcine small intestine to create polymeric intestinal replicas containing biomimetic irregular, multi-scale structures. These replicas were used as molds for polydimethylsiloxane (PDMS) growth substrates with macro to submicron intestinal topographical features. Resultant PDMS replicas exhibit multiscale resolution including macro- to micro-scale folds, crypt and villus structures, and submicron-scale features of the underlying basement membrane. After 10 days of human epithelial colorectal cell culture on PDMS substrates, the inclusion of biomimetic topographical features enhanced alkaline phosphatase expression 2.3-fold compared to flat controls, suggesting biomimetic topography is important in induced epithelial differentiation. This work presents a facile, inexpensive method for precisely replicating complex hierarchal features of native tissue, towards a new model for regenerative medicine and drug delivery for intestinal disorders and diseases.

**Corresponding Author:** Rebecca L. Carrier: Northeastern University, Chemical Engineering, Boston, Massachusetts, USA. Fax: (617) 373-2209; Tel: (617) 373-2989; r.carrier@neu.edu.

**Keywords**

Chemical vapor deposition; Parylene C mold; biomimetic PDMS replica; intestinal epithelium; intestinal tissue engineering

## 1. Introduction

Diseases associated with the small intestine, such as inflammatory bowel disease (IBD) impact millions of people in the United States annually [1]. An added 10,000 patients also suffer from short bowel syndrome (SBS), a malabsorption disorder with high mortality rates following surgical removal of the small intestine [2]. These diseases are often managed via therapeutic interventions that mitigate symptoms, such as immunosuppressants and corticosteroids, however these treatments are not cures [3, 4]. Therefore, it is necessary to develop alternative methods and therapeutics to improve quality of life for the millions of patients suffering from debilitating gastrointestinal disorders.

Cultured intestinal models can facilitate study of these diseases and development of potential new therapies. Traditional intestinal culture models utilize simple 2D monolayers of the human colon carcinoma cell line Caco-2 as an *in vitro* surrogate for human epithelium [5–7]. While these systems have proven useful for study of intestinal function and drug permeation, they lack key features of native intestine, including multiple primary cell types (e.g., paneth cells) and the complex 3D topographical environment of the native small intestine. Recent advances have enabled long-term primary intestinal cultures in the form of three dimensional (3D) organoids [8–12], but culture of primary small intestinal cells as a monolayer, which would facilitate intestinal transport studies, has been limited [8]. Substrates providing complex cues of the native biological milieu, including structural cues, may benefit primary intestinal monolayer cultures.

In the native environment, the epithelium of the small intestine is a tight monolayer in contact with underlying basement membrane supported by the stroma, and is located near capillaries that transport nutrients. The basement membrane is composed of complex, irregular, 3D features over multiple length scales, including macroscopic folds, villi approximately 50–150 μm wide and 100–200 μm tall, crypts 20–50 μm in diameter, 1–5 μm pores, and extracellular matrix (ECM) fibers, such as collagen, that are approximately 50 nm in diameter [13, 14]. *In vivo,* these 3D ECM meshes provide structural support and guide cells [15, 16]. Folds and crypt-villus units increase surface area for absorption of nutrients. The potential significance of these structures to cell phenotype is supported by the specific locations of stem cells and paneth cells in self-renewing crypt-villus units [17]. The micro- and nanometer scale topographies of ECM influence cell phenotype through a variety of mechanisms. Topographical cues are known to impact cell adhesion, ligand distribution and local concentration, integrin interactions, and spatial distribution, which in turn can affect cell-cell contacts, signaling, and responses to local mechanical stress [18–24]. Thus, the intricate multi-scale intestinal structures and known significance of structure to cell function [25–28] motivates the exploration of substrates that incorporate multi-scale topography that mimics the native intestinal niche for improved control of cell phenotype in culture.

In order to present topographical features on cellular growth substrates, various methods have been investigated [29]. Most commonly, micro- and nanofabrication methods, such as photolithography [30], electron-beam lithography [31], two-photon polymerization [32], microcontact printing [32–34], and chemical or electrochemical etching [32] have been employed. These techniques allow fabrication of highly regular and repetitive surface features including microgrooves and ridges [35–37], microwells [38–40], nanoscale roughness [41, 42], and fibers [27, 41, 43–50]. These conventional techniques have been utilized in a variety of applications ranging from improving bone-implant integration [51] to manipulation of neural cell outgrowth [52]. Substrates with structures mimicking intestinal villi [53–56] and crypts [40, 57, 58] have also been fabricated using lithographic techniques. However, these techniques are generally best suited to pattern regular surface features that only approximate aspects of the irregular and multi-scale topography of native tissue. Native intestinal tissue [59] along with multiple other tissue types [16], has been decellularized and used as a substrate. While decellularized tissues certainly present precise structural cues of native tissue, they also present numerous undefined chemical cues.

In an effort to precisely replicate the complex and irregular topography of the small intestine, we have investigated chemical vapor deposition (CVD) to create biocompatible and tunable polymer films for use as growth substrates [58]. CVD is a technique used extensively in the semiconductor industry in which gaseous precursors are introduced under high vacuum, and an initiated chemical reaction produces a thin film on substrates within the reaction chamber [60]. CVD allows for the deposition of conformal films on complex geometries, and chemistries that can be easily manipulated. This technique avoids the surface tension effects of liquid polymer methods that could cause complications when replicating complex biological tissue structures. For example, Cook and colleagues demonstrated the replication of the complex nano- to micro-scale structure of a butterfly wing with CVD of a 100–150 nanometer thick coating of silica followed by thermal removal of tissue [61]. Previous work in our laboratory has shown that CVD of silica can be used to mimic topography of the intestinal basement membrane over multiple length scales. However, due to the brittle, fragile nature of the material, the silica intestinal replicas were unsuitable for use as cellular growth substrates, or to serve as molds for casting materials with native intestinal structure [40, 62]. Thus, to enable replication of multi-scale, complex irregular structure in a growth substrate, an alternative material for creating tissue replicas was sought that: i. could be deposited on tissue via CVD at a rate adequate for creation of micron-thickness films (for mechanical stability upon removal of tissue), ii. would remain chemically stable upon extended immersion in bleach (for removal of underlying tissue), iii. possessed mechanical properties, in the form of a deposited film, suitable for serving as a mold for biocompatible growth substrates. Herein, the ability of CVD of Parylene C to accurately replicate the micro- to nano-scale topography of native porcine small intestine extracellular matrix in a mechanically stable mold was explored. Parylene molds were used for solution casting intestinal replicas using polydimethylsiloxane (PDMS), and the ability of intestinal epithelial cells (Caco-2) to be cultured as a monolayer on complex, irregular topography was demonstrated. Cell morphology and enzymatic activity in culture on biomimetic replicas relative to flat controls were assessed. Biomimetic growth substrates

precisely mimicking the multi-scale topography of intestinal tissue may improve current 2D platforms for drug discovery and regenerative medicine applications.

## 2. Materials and Methods

### 2.1 Intestinal tissue preparation

An overview of the procedure for utilizing native tissue to fabricate replicas is shown in Figure 1. Fresh porcine intestine was received shortly after slaughter from a local abattoir. Full-thickness samples of intestine were cut into approximately 1×3 inch segments, followed by primary fixation with 1% glutaraldehyde (Sigma Aldrich) and 1% paraformaldehyde (Sigma Aldrich) in a 0.1M phosphate buffered saline (PBS; Fisher Scientific) (pH 7.3) solution at 4°C overnight. Samples were cut into smaller pieces (~1 $cm^2$) and were rinsed in PBS for 1 hour. The fixed tissue was then placed in 0.1% osmium tetroxide ($OsO_4$; Sigma Aldrich) in 0.1M PBS at 4°C for 96 hours and shaken in PBS to rinse, followed by sonication to remove all epithelial cellular material while leaving extracellular matrix intact [62]. Samples were then rinsed three times in distilled water over 48 hours, dehydrated using a graded ethanol series, and critical point dried (CPD) using a Samdri®-PVT-3D drier at 40°C and 1200 psi. CPD was utilized as this process dries tissues, for ease of handling, while maintaining tissue topography [62]. Following CPD, samples were stored in a vacuum desiccator until chemical vapor deposition.

### 2.2 Chemical vapour deposition of Parylene

A 10 micron thick film of Parylene C was deposited on fixed and CPD porcine intestinal basement membrane using a PDS 2010 Labcoater 2 Parylene-C Deposition System (Specialty Coating Systems). Chemical vapor deposition (CVD) of Parylene was performed using 20 grams of Parylene at 25 mTorr and 25°C for 8 hours using manufacturer's protocol (690°C, 135°C chamber gauge, 175°C vaporizer, and 35 mTorr). The Parylene deposition process used has three different stages, as previously described [63].

### 2.3 Isolation of Parylene replica from the tissue

Following CVD of Parylene on the intestinal membrane, the tissue was removed by bleach immersion (Reagent Grade, Sigma Aldrich) for ~60 minutes on a stir plate at 60°C. The Parylene replica was then soaked in distilled water for one hour at room temperature to remove residual bleach, and baked at 60°C for 1 hour to dry. Parylene replicas were stored under vacuum in a desiccator until imaging or replica molding.

### 2.4 Positive PDMS replica prepared from negative Parylene mold for cell culture

The side of the Parylene replica that had been in contact with intestinal tissue, containing a negative pattern of native intestinal tissue was used as a mold for creation of PDMS replicas. The Parylene mold was sputter coated with ~10nm gold/palladium (108 Auto Sputter, Ted Pella Inc.) to increase mechanical integrity and aid in separation from the PDMS. Following coating, Parylene mold was silanized under vacuum overnight with hexamethyldisilazane (HMDS; Sigma Aldrich) to aid separation of the polymers. A 10:1 (w:w, PDMS: crosslinker; SYLGARD 184 Dow Corning) PDMS coating was then carefully pipetted over the Parylene mold. Samples were placed in vacuum overnight to degas and then cured at

70°C for 30 minutes. The Parylene-PDMS composite was then separated via differential swelling using triethylamine (TEA; Sigma Aldrich) overnight. The Parylene and PDMS were washed in 100% ethanol for 12 hours, followed by rinsing for 5 minutes in distilled water, and a final rinse in distilled water for 12 hours. PDMS replicas were placed in an oven for 20 minutes at ~65°C to dry prior to storage in a vacuum desiccator until use as cellular growth substrates or for imaging.

### 2.5 Caco-2 cell culture on positive PDMS replica

Prior to culturing of cells, PDMS replicas and flat PDMS control surfaces were oxygen plasma treated using a bench top plasma cleaner (March PX-250) at 50 mW with 8% oxygen for 30 seconds to increase hydrophilicity of the polymer. Samples were then coated with fibronectin solution at a concentration of 50 μg/mL (Bovine, Sigma Aldrich) for 1 hour at room temperature to aid adhesion. Human colorectal epithelial cells, Caco-2 (HTB-37; ATCC), were grown in Eagle's minimum essential medium (EMEM: Gibco) containing 20% fetal bovine serum (FBS; ATCC) and 1% antibiotic-antimitotic solution (10,000 units penicillin, 10 mg streptomycin, and 25 mg amphotericin B per ml, Sigma-Aldrich). Cells were seeded at a density of 76,000 cells/well in a 24-well plate (Falcon; Fisher Scientific) on replicas and flat controls and allowed to grow for 10 days prior to characterization. Medium was replaced every other day.

### 2.6 Fluorescent staining and imaging

Samples were fixed with 4% paraformaldehyde in PBS for 30 minutes at room temperature. Fixed samples were rinsed three times with PBS and permeabilized for 30 minutes with 0.1% Triton X-100 (Sigma Aldrich) in PBS. All samples were then blocked to prevent background staining with 2.5% goat serum (GS) in PBS (Invitrogen) for 1 hour at room temperature.

Alexa-Fluor 546 Phalloidin (Life Technologies) (1:1000 in 2.5% GS) was utilized to visualize filamentous actin and Hoechst 33258 (Molecular Probes) (1:1000 in 2.5% GS) was used to label cell nuclei. Samples were incubated for 1 hour at room temperature and rinsed thrice with PBS. Prolong Gold Anti-fade (Life Technologies) was added and samples were stored at 4°C for less than 24 hours prior to imaging. Samples were imaged with a Nikon A1R confocal microscope in galvano mode at 20x in the Swanson Biotechnology Center imaging core at the Massachusetts Institute of Technology.

### 2.7 Alkaline phosphatase (ALP) and bicinchoninic acid assay (BCA)

An assay for alkaline phosphatase (ALP) activity, an indicator of differentiation, was performed on Caco-2 cell lysates utilizing an ALP detection kit from QuantiChrom™. Samples were washed twice with PBS and lysed with CelLytic™ M cell lysis/extraction reagent (Sigma Aldrich) for 30 minutes at 37°C. Cell lysates were then collected, centrifuged for 15 minutes at 16,000 × g and split into two groups for the bicinchoninic acid assay (BCA), to measure total protein content, and the ALP assay.

Total protein content of the centrifuged samples was calculated via a BCA™ protein assay kit (Pierce). In brief, 200 μL of working reagent (BCA™ reagent A and reagent B at 50:1

ratio) were added to 25 μL of cell lysate, and samples were incubated at 37°C for 30 minutes. After cooling to room temperature, the absorbance of the samples was measured at 562 nm (Bio-Tek Powerwave XS) and compared to a bovine serum albumin (BSA) standard curve for normalization between groups.

For the ALP assay, p-nitrophenyl phosphate (pNPP) was used as the substrate per manufacturer's protocol. In brief, 150 μL of buffered 10 mM pNPP was mixed with 50 μL cell lysate. The absorbance of the solution was recorded at 405 nm every minute for 20 minutes following manufacturer's protocol. The absorbance per minute was calculated using the linear rate region. ALP activity was expressed in units, where 1 unit is equal to the μM of pNPP hydrolyzed per minute and normalized to protein concentration identified via BCA. Samples from three separate experiments, with a minimum of three replicas per condition (flat control versus topographical replica), were analyzed. Statistical significance was determined using the Excel 2010 Analysis ToolPak to perform a two-way ANOVA with replication. Statistical significance was indicated by $p$-values < 0.05.

### 2.8 Characterization of surface topography using scanning electronic microscopy (SEM)

Comparative scanning electron microscopy (SEM) of native tissue and replicated material (Parylene and PDMS) was used to determine the degree of replication of the native intestinal topography. SEM was also used to verify the removal of the epithelium from the native porcine intestinal tissue via osmication, as previously described [58]. SEM images were captured using the Hitachi S-4800 field emission scanning electron microscope (Hitachi Japan) operated at 2 kV. All samples were sputter-coated with a gold-palladium coating of 5–10 nm (40 seconds) thickness, and then secured on conductive sample stands with carbon tape. Further, graphite paint was used to fix the samples on the sample holder to increase conductivity. The working distance was 8mm and a mix of the secondary electron detector and backscattered electron detector was used to obtain the images using fast or slow scan to increase resolution. Quartz PCI software (Quartz Imaging Corporation) was then used to save the images.

## 3. Results

### 3.1 Fixation of native porcine small intestine

In order to make a template for epithelial growth substrates, native porcine small intestine was fixed and osmicated to remove the epithelium, while retaining underlying basement membrane topographical features. Following osmication, scanning electron microscopy (SEM) images indicate removal of epithelium, and reveal a complex multi-scale topography in the native tissue including crypt and villus structures (Figure 2). Incomplete osmication (< 96 hours) can result in remaining epithelium that blocks features, including crypts, during replica molding (Supplemental Figure 1).

### 3.2 Chemical vapor deposition of Parylene as a mold material

Following critical point drying (CPD) of the small intestinal tissue (Figure 3 left), chemical vapor deposition (CVD) was utilized to uniformly apply a layer of Parylene, and bleach was used to remove tissue from the underside of the Parylene (Figure 3 center, top view shown).

The bleach removal process resulted in a freestanding, mechanically stable Parylene replica (Figure 3, Supplemental Figure 2) retaining the complex macroscopic and microscopic topography of the native tissue (Figure 4 A, C). Microscopic villus features dominating the surfaces of osmicated native tissue (Figure 4 A, C) are also apparent on Parylene replicas (Figure 4 B, D). This approach was explored with the intention of using the resulting Parylene mold for recasting multiple replicas of the biological topography in a biocompatible material. However, examination at higher magnification revealed that the Parylene deposition process on the intestine resulted in "island domain" features on the top of the Parylene replica that masked some smaller structures, limiting use of this surface as a mold (Figure 4 E, F). Therefore, to utilize Parylene as a mold for a growth substrate, the underside of the Parylene replica that had been in contact with intestinal tissue was used as a "negative" Parylene mold to create a "positive" PDMS replica (Figure 1; Supplemental Figure 2).

### 3.3 Replica molding of PDMS growth substrate from Parylene mold

Following creation of Parylene molds of small intestinal tissue, to create a reusable growth substrate, negative Parylene molds (surfaces that were in contact with native tissue prior to bleach treatment) were sputter coated with gold palladium (~10 nm thick) to increase rigidity for handling. PDMS was then solution cast within the negative Parylene molds to create a positive replica to use as a growth substrate. Separation of the negative Parylene mold and the polymerized positive PDMS replica was achieved via soaking in triethylamine (TEA). This method is commonly used in soft lithography to separate complex features, as TEA induces a swelling of PDMS, which upon rinses and baking returns to its original size [64–66]. Physically peeling apart the Parylene mold and PDMS replica while maintaining their integrity without the use of TEA was not successful (not shown) due to the high surface area and complex, high aspect ratio features.

PDMS replicas macroscopically appear similar to native tissue (Figure 3). Higher magnification comparisons of the topographical structures of the native tissue (Figure 5 A–C) with negative Parylene mold (Figure 5 D–F) and positive PDMS replica (Figure 5 G–I) indicates transfer of structural features. The native tissue exhibits millimeter-scale folds that translate to valleys in Parylene, and folds in the positive PDMS. Villi on the scale of hundreds of microns in tissue translate to depressions in the Parylene and PDMS projections closely resembling native villus structures. Thus, the macro- to micro-scale features were preserved during the CVD process and solution replica casting of the PDMS onto the Parylene. The presence of crypts at the base of the villi is apparent and matches projections on the negative mold created with the Parylene replicas.

SEM images at higher magnifications indicate replication of intestinal basement membrane features in the negative Parylene mold and positive PDMS replica down to the submicron scale (Supplemental Figure 3). For example, in the native small intestinal tissue, pores approximately 1–5 microns in size, and ECM protein fibers forming linear structures less than a micron in diameter are apparent (Supplemental Figure 3A). In the final PDMS replica, there are regions of linear topographical features at a similar size scale as fibrous features on the native tissue (Supplemental Figure 3B), including pore-like features. There is

a loss of resolution in the overall complexity and number of features that are transferred across replica molding steps.

### 3.4 Cell culture and alkaline phosphatase expression on PDMS replicas of intestinal basement membrane

Epithelial cells (Caco-2) were seeded on the complex 3D surface topography on the biomimetic topographical replicas. Confocal microscopy indicates that after 10 days in culture, epithelial cells form confluent monolayers on both the flat control PDMS substrates and substrates containing the topographical replicas (Figure 6). Caco-2 on the flat PDMS surface grow in a distinct flat monolayer, while on the topographical replicas the Z height of the cellular monolayer varies along with the topography. Visually, the morphology of the Caco-2 is also modified on the biomimetic PDMS growth substrates. On flat PDMS, the nuclei are larger and rounded; while on the topographical replicas the majority of nuclei are narrower and appear columnar, indicating a more mature phenotype [67]. Due to the presence of macro-scale features (> 1mm) of the replicated native tissue folds in the PDMS and confocal microscopy working distance limitations, it was not possible to capture Z-stacks that encompassed the entirety of the topographical replicas. This limitation resulted in cellular regions being outside the capture area and resultant dark regions in the topographical replica images. However, manual focusing in different planes confirms culture of a confluent monolayer on the complex structures.

As an initial investigation of the maturity of the epithelial cells cultured on the replicas and flat controls, activity of alkaline phosphatase (ALP), a brush border enzyme, was measured as an indicator of Caco-2 differentiation. After 10 days of growth in standard culture conditions, ALP activity was significantly increased (2.3-fold) on biomimetic PDMS growth substrates compared to flat PDMS control growth substrates (Figure 7, $p<0.05$), indicating an influence of topography on Caco-2 differentiation [67–69].

## 4. Discussion

The prevalent culture model for intestinal epithelium utilizes Caco-2 cells grown on 2D Transwell™ membranes [70]. However, flat growth substrates lack the complex topographical cues of the native small intestinal niche that may impact cell phenotype. Herein, we describe for the first time a facile method to create polymeric growth substrates precisely mimicking the complex, 3D, irregular features of the native small intestine through chemical vapor deposition (CVD) and replica molding. The protocol described could be easily translated to create precise biomimetic replicas of other tissue surfaces, especially other epithelial tissues. This method recapitulated macro- to submicron-scale structures of the small intestinal basement membrane, including villi. Confocal images show that seeded cells divide and/or migrate into the depressions and up the villus projections of the intestinal replica, forming a confluent monolayer over these complex features. Epithelial cells grown on biomimetic substrates were found to have higher levels of alkaline phosphatase activity, an indicator of differentiation, after 10 days compared to cells grown on flat controls. Providing a biomimetic growth substrate that mimics the topography of the native intestine may impact epithelial phenotype.

Previous investigations of the impact of topography on epithelial cells have provided important insight into cell behavior, but have been mainly limited to substrates with repetitive or random topographical cues. For example, Andersson and colleagues found that compared to flat controls, bladder epithelial cell morphology and interleukin expression were impacted by culture on titanium oxide surfaces with regularly patterned microgrooves created via photolithography, indicating the underlying topography impacts epithelial phenotype [71]. Corneal epithelial cells grown on polyurethane substrates with feature sizes similar to collagen fibrils (200–2000 nm) exhibited increased proliferation [42], and those grown on topographically modified functionalized polyethylene glycol diacrylate (PEGDA) gels aligned with ridges [72]. Pins and colleagues fabricated polydimethylsiloxane (PDMS) substrates with grooves (40 – 310 $\mu M$ width) as templates for collagen films topographically mimicking the native basal lamina [73]. Keratinocytes grown *in vitro* on these collagen analogues formed a stratified, differentiated epidermis, with topography impacting differentiation as evidenced by greater stratification in deeper channels. Using lithographic techniques, Teixeira and colleagues fabricated substrates with ridges and grooves as small as 70 nm, and found corneal epithelial cells took on an elongated morphology when cultured on grooved substrates compared to flat controls [74]. Topography has also been shown to impact epithelial migration, with cells migrating along grooves and ridges (400–4000 nm) created via lithography and ion etching [75], and migration impacted by micro-pit and -pillar structures [76]. It was also demonstrated using micro-patterned silk films that corneal-limbal epithelial sheet migration, in addition to migration of individual cells, can be directed using topographical cues [77]. Topographical features have also been used to study epithelial cell behaviors associated with cancer, including metastatic invasiveness of mammary epithelial cells induced by microfabricated collagen tracks [78] and epithelial-mesenchymal transition (EMT) of human MCF-7 enhanced on aligned electrospun poly-lactic acid (PLA) [79]. Lithographic techniques were also used to recreate micro-wells mimicking crypt structures [40, 57] and projections closely resembling villus structures [53, 80] in polymeric substrates, and it was demonstrated that culture on these patterned substrates impacted intestinal cell differentiation. While promising for multiple tissue engineering applications, conventional microfabrication techniques such as those described above are unable to recreate the complex, irregular structures of the small intestine ranging from macro-scale folds to sub-micron scale fibrous structures presented by extracellular matrix proteins. Intestinal tissue has been decellularized such that villus and crypt architecture remained intact and resulting matrices could support cultured cells [59]. However, it may be desirable to recreate multiscale irregular intestinal structures in a polymeric substrate to avoid undefined chemistry and variability of biological specimens.

In this work, CVD was used to recreate the irregular surface topography of the small intestine [25, 81]. The process of CVD allows conformal coating of features down to the nanoscale through uniform film deposition directly onto substrates [28]. Previous work in our lab employed CVD of silica on osmicated small intestinal tissue to precisely mimic irregular topography in rigid silica substrates down to the micron scale [62]. While these results were promising, the brittle nature of the silica substrates limited their utility in molding processes, motivating exploration of reusable and more robust polymeric molds for

creating epithelial cell growth substrates. CVD of the polymer Parylene was thus investigated for the replication of small intestinal basement membrane topography.

Parylene is a hydrophobic and biocompatible polymer that has been shown to be suitable for cell culture [82]. Parylene films can also be used as stencils for patterning different cell types [83]. To create a reusable mold for casting growth substrates, a 10-μm thick Parylene film was deposited on osmicated intestinal tissue. After bleach removal of the porcine intestinal tissue, the resulting freestanding Parylene replica was examined via SEM, and results show the complex and irregular topography of native small intestine can be recreated via CVD of Parylene (Figures 4). However, the positive Parylene replicas were limited in use as growth substrates due to the polymer coating masking underlying topographical features.

In order to create a “positive” growth substrate with topography of the small intestine from “negative” Parylene molds, PDMS was chosen due to its physical properties of transparency, tunable elasticity, inertness, and low cost [26]. PDMS based scaffolds have been successfully utilized for replica molding of glial cell topography to manipulate neuronal extension [84]. It was demonstrated that Parylene molds could act as reusable templates for casting structurally biomimetic PDMS culture substrates. SEM images (Figure 5) show the ability of CVD of Parylene and resultant PDMS growth substrates to recapitulate the complexity of the native tissue on multiple scales. Villus protrusions are evident on the order of approximately 200 microns. These features are important in epithelial culture, as in the native environment differentiated enterocytes locate to villus tips to absorb nutrients, and shed into the lumen over time [85]. In this work, while the presence of crypt features at the base of villi was apparent (Figure 5), there was some residual cellular debris in some crypt openings. Therefore, the limitations of this method likely lay with the original preparation of the native tissue itself, and not the CVD process. Increasing agitation and rinsing steps during and post-osmication may improve reproducibility of mimicking basement membrane structural features. Inclusion of crypt structures in a growth substrate should be considered, in particular for the culture of primary cells, as stem cells and paneth cells localize in crypts *in vivo*. One potential effect of crypt and villus structures may be increasing proximity of apical surfaces of cells, thus facilitating paracrine signaling in the intestinal niche [82, 86].

At the submicron scale, the native small intestinal basement membrane is composed of fibrous matrix proteins and pores less than 5 μM in size (Supplemental Figure 3). Final solution casted PDMS growth substrates exhibit some linear features on the size scale of fibrous proteins apparent in the native tissue. While the replica molding process fails to recreate the entire complexity of the native topography, some aspects of the nanoscale features appear to remain.

Further, these complex biomimetic growth substrates were shown to support formation of conformal Caco-2 monolayers (Figure 6). Confocal microscopy was utilized to image through the PDMS replicas, and height variations in the topographical replica (Figure 6B) are seen in the orthogonal view while the flat surface is shows a smooth monolayer (Figure 6A). The polymer replica exhibits a high light refraction due to macro and microscopic structural features, limiting the resolution of the microscopy. Alkaline phosphatase

expression was significantly enhanced on topographical replicas compared to flat PDMS control growth substrates after 10 days (Figure 7) [87]. Our lab previously developed repetitive micro-well (10–500 micron diameter) patterns designed to approximately mimic crypt structures using lithographic techniques, and demonstrated that Caco-2 cells cultured on the micro-well patterns had higher mitochondrial activity but lower alkaline phosphatase activity compared to flat substrates, indicating a less mature phenotype [40]. It is interesting that lower levels of brush boarder enzyme activity were observed on crypt-like structures, and less differentiated cells reside in crypts *in vivo*, while in this work we observed higher levels of alkaline phosphatase on surfaces dominated by villus-like protrusions, consistent with more differentiated cells residing on villi *in vivo*.

## 5. Conclusion

*In vivo*, cells are surrounded by and in direct contact with 3D ECM, which often possesses rich micro- and nano-scale topography that impacts cell phenotype. In this study, CVD was used to create thin films of Parylene C and solution casted PDMS to replicate the complex and multi-scale topography of the small intestinal basement membrane in a growth substrate. CVD of Parylene C produced replicas of the small intestine with features down to the submicron scale. Solution cast PDMS from the primary Parylene replica also demonstrated features similar to native intestinal tissue including macro-scale folds, crypts and villi, as well as some features of the fibrous underlying basement membrane. Epithelial alkaline phosphatase activity was significantly enhanced by culture on PDMS replicas relative to culture on flat controls. These results support the influence of biomimetic scaffold topography on epithelial phenotype and present a robust, repeatable, facile method for precisely replicating irregular biological topography in cell culture substrate materials. The developed process would allow for rapid development of multiple topographically biomimetic polymeric cell culture substrates from a single biological specimen. This work has broad implications for model systems for drug discovery and regenerative medicine. Ongoing work involves investigating the functionality and behavior of primary small intestinal enteroids cultured on structurally biomimetic films and hydrogels towards creation of a platform for primary small intestine epithelial culture.

## Acknowledgements

The authors thank members of the Carrier laboratory and funding from the NIH (R21EY021312), NSF (CBET #0700764 and CMMI #0727984) (RLC) and an NSF ADVANCE Future Faculty Fellowship (ANK). We also thank Eliza Vasile of the Swanson Biotechnology Center imaging core at Massachusetts Institute of Technology for her help with microscopy.

## References

1. Park K, Bass D. Inflammatory bowel diseaseattributable costs and costeffective strategies in the United States: A review. Inflammatory Bowel Diseases. 2011;17(7):1603–9. [PubMed: 21053357]
2. Buchman AL. Etiology and initial management of short bowel syndrome. Gastroenterology. 2006;130(2 Suppl 1):S5–S15. [PubMed: 16473072]
3. Faubion WA Jr, Loftus EV Jr, Harmsen WS, Zinsmeister AR, Sandborn WJ. The natural history of corticosteroid therapy for inflammatory bowel disease: a population-based study. Gastroenterology. 2001;121(2):255–60. [PubMed: 11487534]

4. Khan KJ, Dubinsky MC, Ford AC, Ullman TA, Talley NJ, Moayyedi P. Efficacy of immunosuppressive therapy for inflammatory bowel disease: a systematic review and meta-analysis. The American journal of gastroenterology. 2011;106(4):630–42. [PubMed: 21407186]
5. Yee S In vitro permeability across Caco-2 cells (colonic) can predict in vivo (small intestinal) absorption in man—fact or myth. Pharmaceutical research. 1997;14(6):763–6. [PubMed: 9210194]
6. Hidalgo IJ, Raub TJ, Borchardt RT. Characterization of the human colon carcinoma cell line (Caco-2) as a model system for intestinal epithelial permeability. Gastroenterology. 1989;96(3):736–49. [PubMed: 2914637]
7. Artursson P, Palm K, Luthman K. Caco-2 monolayers in experimental and theoretical predictions of drug transport. Advanced drug delivery reviews. 2001;46(1):27–43. [PubMed: 11259831]
8. Moon C, Vandussen K, Miyoshi H, Stappenbeck T. Development of a primary mouse intestinal epithelial cell monolayer culture system to evaluate factors that modulate IgA transcytosis. Mucosal immunology. 2013;7:818–28. [PubMed: 24220295]
9. Yu J, Carrier RL, March JC, Griffith LG. Three dimensional human small intestine models for ADME-Tox studies. Drug discovery today. 2014;19.10:1587–94. [PubMed: 24853950]
10. Jung P, Sato T, Merlos-Suarez A, Barriga FM, Iglesias M, Rossell D, et al. Isolation and in vitro expansion of human colonic stem cells. Nature Medicine (New York, NY, United States). 2011;17(10):1225–7.
11. Sato T, Stange DE, Ferrante M, Vries RGJ, van Es JH, van den Brink S, et al. Long-term Expansion of Epithelial Organoids From Human Colon, Adenoma, Adenocarcinoma, and Barrett's Epithelium. Gastroenterology. 2011;141(5):1762–72. [PubMed: 21889923]
12. Sato T, van Es JH, Snippert HJ, Stange DE, Vries RG, van den Born M, et al. Paneth cells constitute the niche for Lgr5 stem cells in intestinal crypts. Nature (London, United Kingdom). 2011;469(7330):415–8. [PubMed: 21113151]
13. Takahashi-Iwanaga H, Iwanaga T, Isyama H. Porosity of the epithelial basement membrane as an indicator of macrophage-enterocyte interaction in the intestinal mucosa. Archives of histology and cytology. 1999;62(5):471–81. [PubMed: 10678576]
14. Takeuchi T, Gonda T. Distribution of the pores of epithelial basement membrane in the rat small intestine. The Journal of veterinary medical science. 2004;66(6):695–700. [PubMed: 15240945]
15. Gilbert TW, Sellaro TL, Badylak SF. Decellularization of tissues and organs. Biomaterials. 2006;27(19):3675–83. [PubMed: 16519932]
16. Badylak SF. Xenogeneic extracellular matrix as a scaffold for tissue reconstruction. Transplant immunology. 2004;12(3):367–77. [PubMed: 15157928]
17. Clevers H The intestinal crypt, a prototype stem cell compartment. Cell. 2013;154(2):274–84. [PubMed: 23870119]
18. Buck CA, Horwitz AF. Cell surface receptors for extracellular matrix molecules. Annual review of cell biology. 1987;3(1):179–205.
19. Roskelley C, Desprez P, Bissell M. Extracellular matrix-dependent tissue-specific gene expression in mammary epithelial cells requires both physical and biochemical signal transduction. Proceedings of the National Academy of Sciences. 1994;91(26):12378–82.
20. Meredith J, Fazeli B, Schwartz M. The extracellular matrix as a cell survival factor. Molecular biology of the cell. 1993;4(9):953–61. [PubMed: 8257797]
21. Frisch SM, Francis H. Disruption of epithelial cell-matrix interactions induces apoptosis. The Journal of cell biology. 1994;124(4):619–26. [PubMed: 8106557]
22. Burridge K, Fath K, Kelly T, Nuckolls G, Turner C. Focal adhesions: transmembrane junctions between the extracellular matrix and the cytoskeleton. Annual review of cell biology. 1988;4(1):487–525.
23. Streuli C Extracellular matrix remodelling and cellular differentiation. Current opinion in cell biology. 1999;11(5):634–40. [PubMed: 10508658]
24. Curtis A, Wilkinson C. Topographical control of cells. Biomaterials. 1997;18(24):1573–83. [PubMed: 9613804]
25. Khademhosseini A, Langer R, Borenstein J, Vacanti JP. Microscale technologies for tissue engineering and biology. Proceedings of the National Academy of Sciences of the United States of America. 2006;103(8):2480–7. [PubMed: 16477028]

26. Roach P, Eglin D, Rohde K, Perry CC. Modern biomaterials: a review—bulk properties and implications of surface modifications. Journal of Materials Science: Materials in Medicine. 2007;18(7):1263–77. [PubMed: 17443395]
27. Bettinger CJ, Langer R, Borenstein JT. Engineering substrate topography at the micro- and nanoscale to control cell function. Angewandte Chemie International Edition England. 2009;48(30):5406–15.
28. Ma PX. Biomimetic materials for tissue engineering. Advanced drug delivery reviews. 2008;60(2):184–98. [PubMed: 18045729]
29. Park J, Kim P, Helen W, Engler AJ, Levchenko A, Kim D-H. Control of stem cell fate and function by engineering physical microenvironments. Integrative Biology. 2012;4(9):1008–18. [PubMed: 23077731]
30. Charest JL, Eliason MT, García AJ, King WP. Combined microscale mechanical topography and chemical patterns on polymer cell culture substrates. Biomaterials. 2006;27(11):2487–94. [PubMed: 16325902]
31. Dalby MJ, Gadegaard N, Wilkinson CD. The response of fibroblasts to hexagonal nanotopography fabricated by electron beam lithography. Journal of Biomedical Materials Research Part A. 2008;84(4):973–9. [PubMed: 17647239]
32. Ovsianikov A, Schlie S, Ngezahayo A, Haverich A, Chichkov BN. Twophoton polymerization technique for microfabrication of CAD designed 3D scaffolds from commercially available photosensitive materials. Journal of tissue engineering and regenerative medicine. 2007;1(6):443–9. [PubMed: 18265416]
33. Altomare L, Gadegaard N, Visai L, Tanzi M, Farè S. Biodegradable microgrooved polymeric surfaces obtained by photolithography for skeletal muscle cell orientation and myotube development. Acta biomaterialia. 2010;6(6):1948–57. [PubMed: 20040385]
34. Altomare L, Riehle M, Gadegaard N, Tanzi M, Farè S. Microcontact printing of fibronectin on a biodegradable polymeric surface for skeletal muscle cell orientation. International Journal of Artificial Organs. 2010;33(8):535.
35. Hoffman-Kim D, Mitchel JA, Bellamkonda RV. Topography, cell response, and nerve regeneration. Annual review of biomedical engineering. 2010;12:203.
36. Den Braber E, De Ruijter J, Smits H, Ginsel L, Von Recum A, Jansen J. Effect of parallel surface microgrooves and surface energy on cell growth. Journal of biomedical materials research. 1995;29(4):511–8. [PubMed: 7622536]
37. Dalton B, Walboomers XF, Dziegielewski M, Evans MD, Taylor S, Jansen JA, et al. Modulation of epithelial tissue and cell migration by microgrooves. Journal of biomedical materials research. 2001;56(2):195–207. [PubMed: 11340589]
38. Charnley M, Textor M, Khademhosseini A, Lutolf MP. Integration column: microwell arrays for mammalian cell culture. Integrative Biology. 2009;1(11–12):625–34. [PubMed: 20027371]
39. Broderick AH, Azarin SM, Buck ME, Palecek SP, Lynn DM. Fabrication and selective functionalization of amine-reactive polymer multilayers on topographically patterned microwell cell culture arrays. Biomacromolecules. 2011;12(6):1998–2007. [PubMed: 21504222]
40. Wang L, Murthy SK, Fowle WH, Barabino GA, Carrier RL. Influence of micro-well biomimetic topography on intestinal epithelial Caco-2 cell phenotype. Biomaterials. 2009;30(36):6825–34. [PubMed: 19766306]
41. Pham QP, Sharma U, Mikos AG. Electrospinning of polymeric nanofibers for tissue engineering applications: a review. Tissue engineering. 2006;12(5):1197–211. [PubMed: 16771634]
42. Liliensiek S, Campbell S, Nealey P, Murphy C. The scale of substratum topographic features modulates proliferation of corneal epithelial cells and corneal fibroblasts. Journal of biomedical materials research Part A. 2006;79(1):185–92. [PubMed: 16817223]
43. Mo X, Xu C, Kotaki Mea, Ramakrishna S. Electrospun P (LLA-CL) nanofiber: a biomimetic extracellular matrix for smooth muscle cell and endothelial cell proliferation. Biomaterials. 2004;25(10):1883–90. [PubMed: 14738852]
44. Badami AS, Kreke MR, Thompson MS, Riffle JS, Goldstein AS. Effect of fiber diameter on spreading, proliferation, and differentiation of osteoblastic cells on electrospun poly (lactic acid) substrates. Biomaterials. 2006;27(4):596–606. [PubMed: 16023716]

45. Jin H-J, Chen J, Karageorgiou V, Altman GH, Kaplan DL. Human bone marrow stromal cell responses on electrospun silk fibroin mats. Biomaterials. 2004;25(6):1039–47. [PubMed: 14615169]
46. Deshpande P, McKean R, Blackwood KA, Senior RA, Ogunbanjo A, Ryan AJ, et al. Using poly (lactide-co-glycolide) electrospun scaffolds to deliver cultured epithelial cells to the cornea. Regenerative medicine. 2010;5(3):395–401. [PubMed: 20455650]
47. Lee KY, Mooney DJ. Hydrogels for tissue engineering. Chemical Reviews. 2001;101(7):1869–80. [PubMed: 11710233]
48. Tibbitt MW, Anseth KS. Hydrogels as extracellular matrix mimics for 3D cell culture. Biotechnology and bioengineering. 2009;103(4):655–63. [PubMed: 19472329]
49. Sill TJ, von Recum HA. Electrospinning: applications in drug delivery and tissue engineering. Biomaterials. 2008;29(13):1989–2006. [PubMed: 18281090]
50. Seidlits SK, Lee JY, Schmidt CE. Nanostructured scaffolds for neural applications. Nanomedicine 2008;3(2):183–99. [PubMed: 18373425]
51. Wennerberg A, Albrektsson T. Effects of titanium surface topography on bone integration: a systematic review. Clinical oral implants research. 2009;20(s4):172–84. [PubMed: 19663964]
52. Lee MR, Kwon KW, Jung H, Kim HN, Suh KY, Kim K, et al. Direct differentiation of human embryonic stem cells into selective neurons on nanoscale ridge/groove pattern arrays. Biomaterials. 2010;31(15):4360–6. [PubMed: 20202681]
53. Costello CM, Hongpeng J, Shaffiey S, Yu J, Jain NK, Hackam D, et al. Synthetic small intestinal scaffolds for improved studies of intestinal differentiation. Biotechnology and bioengineering. 2014;111(6):1222–32. [PubMed: 24390638]
54. Sung JH, Yu J, Luo D, Shuler ML, March JC. Microscale 3-D hydrogel scaffold for biomimetic gastrointestinal (GI) tract model. Lab on a Chip. 2011;11(3):389–92. [PubMed: 21157619]
55. Yu J, Peng S, Luo D, March JC. In vitro 3D human small intestinal villous model for drug permeability determination. Biotechnology and bioengineering. 2012;109(9):2173–8. [PubMed: 22488418]
56. Esch MB, Sung JH, Yang J, Yu C, Yu J, March JC, et al. On chip porous polymer membranes for integration of gastrointestinal tract epithelium with microfluidic 'body-on-a-chip'devices. Biomedical microdevices. 2012;14(5):895–906. [PubMed: 22847474]
57. Wang L, Murthy SK, Barabino GA, Carrier RL. Synergic effects of crypt-like topography and ECM proteins on intestinal cell behavior in collagen based membranes. Biomaterials. 2010;31(29):7586–98. [PubMed: 20643478]
58. Pfluger CA, Burkey DD, Wang L, Sun B, Ziemer KS, Carrier RL. Biocompatibility of plasma enhanced chemical vapor deposited poly(2-hydroxyethyl methacrylate) films for biomimetic replication of the intestinal basement membrane. Biomacromolecules. 2010;11(6):1579–84. [PubMed: 20441140]
59. Totonelli G, Maghsoudlou P, Garriboli M, Riegler J, Orlando G, Burns AJ, et al. A rat decellularized small bowel scaffold that preserves villus-crypt architecture for intestinal regeneration. Biomaterials. 2012;33(12):3401–10. [PubMed: 22305104]
60. Ma M, Mao Y, Gupta M, Gleason KK, Rutledge GC. Superhydrophobic fabrics produced by electrospinning and chemical vapor deposition. Macromolecules. 2005;38(23):9742–8.
61. Cook G, Timms PL, Goltner-Spickermann C. Exact replication of biological structures by chemical vapor deposition of silica. Angewandte Chemie International Edition. 2003;42(5):557–9. [PubMed: 12569489]
62. Pfluger CA, McMahon BJ, Carrier RL, Burkey DD. Precise, Biomimetic Replication of the Multiscale Structure of Intestinal Basement Membrane Using Chemical Vapor Deposition. Tissue Engineering Part A. 2012;19(5–6):649–56. [PubMed: 23013380]
63. Selvarasah S, Chao S, Chen C, Sridhar S, Busnaina A, Khademhosseini A, et al. A reusable high aspect ratio parylene-C shadow mask technology for diverse micropatterning applications. Sensors and Actuators A. 2008;145–146:306–15.
64. Rolland JP, Van Dam RM, Schorzman DA, Quake SR, DeSimone JM. Solvent-resistant photocurable "liquid teflon" for microfluidic device fabrication. Journal of the American Chemical Society. 2004;126(8):2322–3. [PubMed: 14982433]

65. Verma MK, Majumder A, Ghatak A. Embedded template-assisted fabrication of complex microchannels in PDMS and design of a microfluidic adhesive. Langmuir. 2006;22(24):10291–5. [PubMed: 17107035]
66. Lee JN, Park C, Whitesides GM. Solvent compatibility of poly (dimethylsiloxane)-based microfluidic devices. Analytical chemistry. 2003;75(23):6544–54. [PubMed: 14640726]
67. Hilgers AR, Conradi RA, Burton PS. Caco-2 cell monolayers as a model for drug transport across the intestinal mucosa. Pharmaceutical research. 1990;7(9):902–10. [PubMed: 2235888]
68. Cell B Enterocyte-like differentiation and polarization of the human colon carcinoma cell line Caco-2 in culture. Biology of the Cell. 1983;47. [PubMed: 6673789]
69. Engle M, Goetz G, Alpers D. Caco-2 cells express a combination of colonocyte and enterocyte phenotypes. Journal of cellular physiology. 1998;174(3):362–9. [PubMed: 9462698]
70. Gan L-SL, Thakker DR. Applications of the Caco-2 model in the design and development of orally active drugs: elucidation of biochemical and physical barriers posed by the intestinal epithelium. Advanced Drug Delivery Reviews. 1997;23(1–3):77–98.
71. Andersson A-S, Bäckhed F, von Euler A, Richter-Dahlfors A, Sutherland D, Kasemo B. Nanoscale features influence epithelial cell morphology and cytokine production. Biomaterials. 2003;24(20):3427–36. [PubMed: 12809771]
72. YañezSoto B, Liliensiek S, Murphy C, Nealey P. Biochemically and topographically engineered poly (ethylene glycol) diacrylate hydrogels with biomimetic characteristics as substrates for human corneal epithelial cells. Journal of biomedical materials research Part A. 2013;101(4):1184–94. [PubMed: 23255502]
73. Pins G, Toner M, Morgan JR. Microfabrication of an analog of the basal lamina: biocompatible membranes with complex topographies. The FASEB Journal. 2000;14:593–602. [PubMed: 10698975]
74. Teixeira AI, Abrams GA, Bertics PJ, Murphy CJ, Nealey PF. Epithelial contact guidance on well-defined micro-and nanostructured substrates. Journal of cell science. 2003;116(10):1881–92. [PubMed: 12692189]
75. Diehl K, Foley J, Nealey P, Murphy C. Nanoscale topography modulates corneal epithelial cell migration. Journal of biomedical materials research Part A. 2005;75(3):603–11. [PubMed: 16106433]
76. Jeon H, Simon CG, Kim G. A minireview: Cell response to microscale, nanoscale, and hierarchical patterning of surface structure. Journal of Biomedical Materials Research Part B: Applied Biomaterials. 2014;102(7):1580–94.
77. Lawrence BD, Pan Z, Rosenblatt MI. Silk film topography directs collective epithelial cell migration. 2012.
78. Kraning-Rush CM, Carey SP, Lampi MC, Reinhart-King CA. Microfabricated collagen tracks facilitate single cell metastatic invasion in 3D. Integrative Biology. 2013;5(3):606–16. [PubMed: 23388698]
79. Foroni L, Vasuri F, Valente S, Gualandi C, Focarete ML, Caprara G, et al. The role of 3D microenvironmental organization in MCF-7 epithelial–mesenchymal transition after 7 culture days. Experimental cell research. 2013;319(10):1515–22. [PubMed: 23583658]
80. Costello CM, Sorna RM, Goh Y-L, Cengic I, Jain NK, March JC. 3-D Intestinal Scaffolds for Evaluating the Therapeutic Potential of Probiotics. Molecular pharmaceutics. 2014;11(7):2030–9. [PubMed: 24798584]
81. Khademhosseini A, Langer R. Microengineered hydrogels for tissue engineering. Biomaterials. 2007;28(34):5087–92. [PubMed: 17707502]
82. Chang T, Yadav V, De Leo S, Mohedas A, Rajalingam B, Chen C, et al. Cell and Protein Compatibility of Parylene-C. Surfaces. Langmuir. 2007;23(23):11718 – 25. [PubMed: 17915896]
83. Jinno S, Moeller H, Chen C, Rajalingam B, Chung B, Khademhosseini A. Microfabricated multilayer parylene-C stencils for the generation of patterned dynamic co-cultures. Journal of Biomedical Materials Research Part A. 2008;86:278 – 88. [PubMed: 18442109]
84. Bruder JM, Monu NC, Harrison MW, Hoffman-Kim D. Fabrication of polymeric replicas of cell surfaces with nanoscale resolution. Langmuir. 2006;22(20):8266–70. [PubMed: 16981733]

85. Reya T, Clevers H. Wnt signalling in stem cells and cancer. Nature (London, United Kingdom). 2005;434(7035):843–50. [PubMed: 15829953]

86. Madison BB, Braunstein K, Kuizon E, Portman K, Qiao XT, Gumucio DL. Epithelial hedgehog signals pattern the intestinal crypt-villus axis. Development. 2005;132(2):279–89. [PubMed: 15590741]

87. Pinto M, Robine-Leon S, Appay MD, Kedinger M, Triadou N, Dussaulx E, et al. Enterocyte-like differentiation and polarization of the human colon carcinoma cell-line (CaCo-2) in culture. Biology of the Cell 1983;47:323–30.

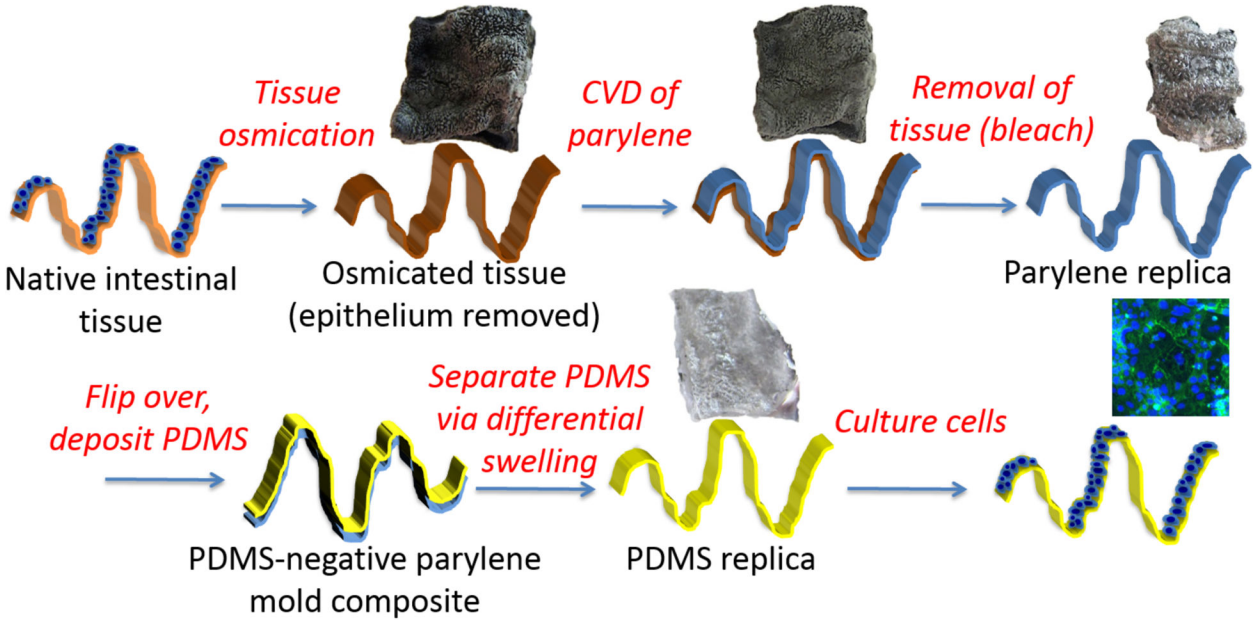


**Figure 1.**

Stepwise process overview for utilizing native small intestinal tissue as a substrate for chemical vapor deposition of a Parylene C mold. The Parylene mold is used to fabricate biomimetic PDMS replicas used as cellular growth substrates.

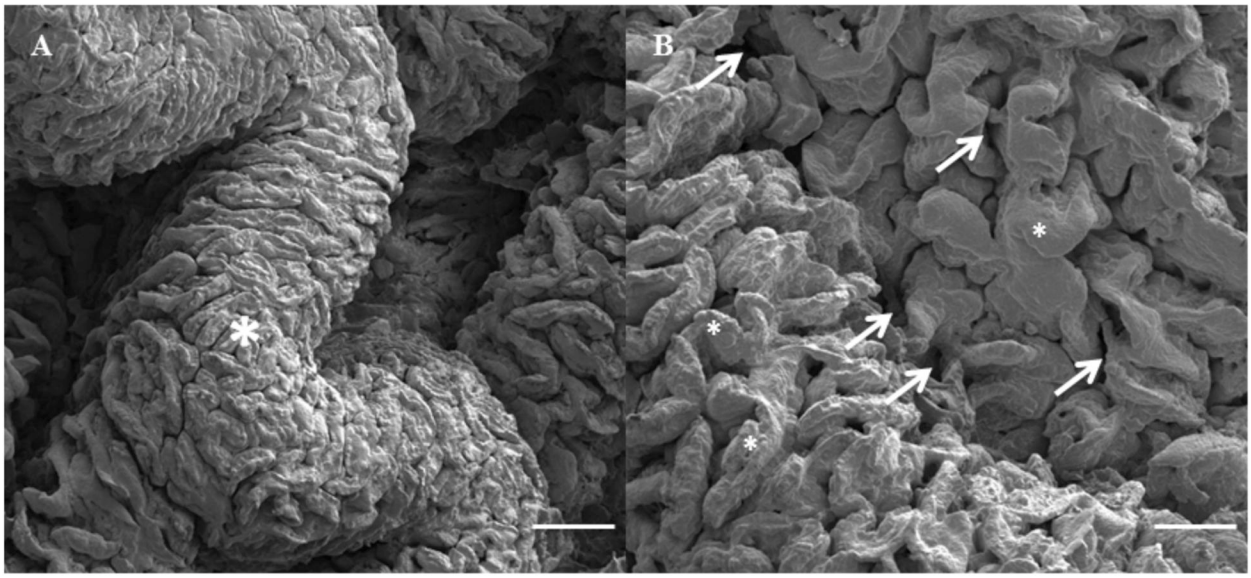


**Figure 2.**

SEM images show varying topographical features of osmium fixed native small intestinal tissue, including (a) macroscopic folds (*) and (b) microscopic villi (*) and crypts (arrows). Bar = 1 mm in (a) and 500 μM in (b).

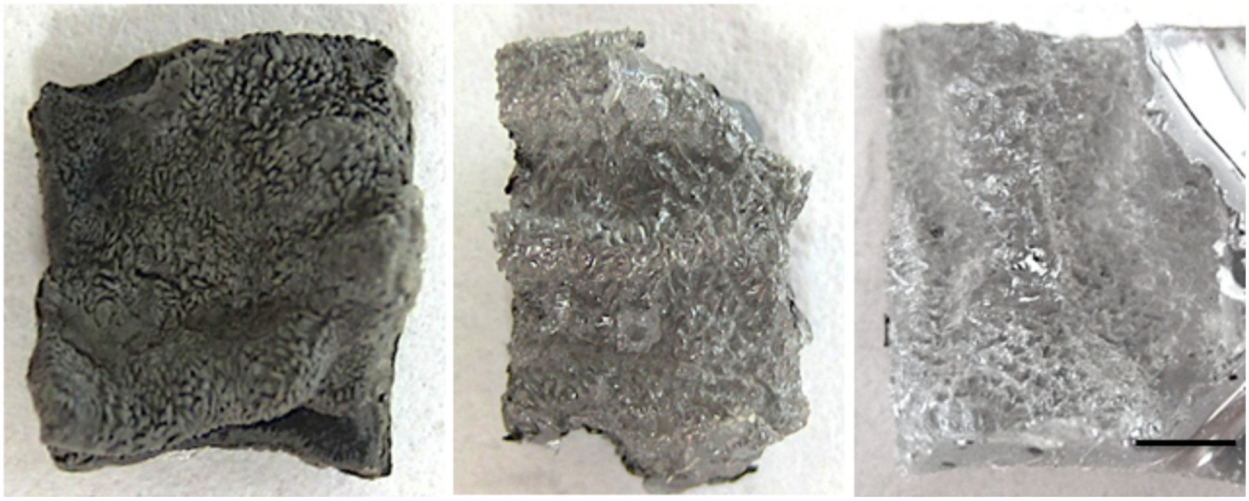

**Figure 3.**

Macroscale photograph of representative osmium fixed native small intestinal tissue (left), CVD positive (top view) Parylene replica (center), and final positive PDMS growth substrate (right). Sputter coated Parylene and PDMS are shown for increased contrast due to transparency of the materials. Bar = 3 mm.

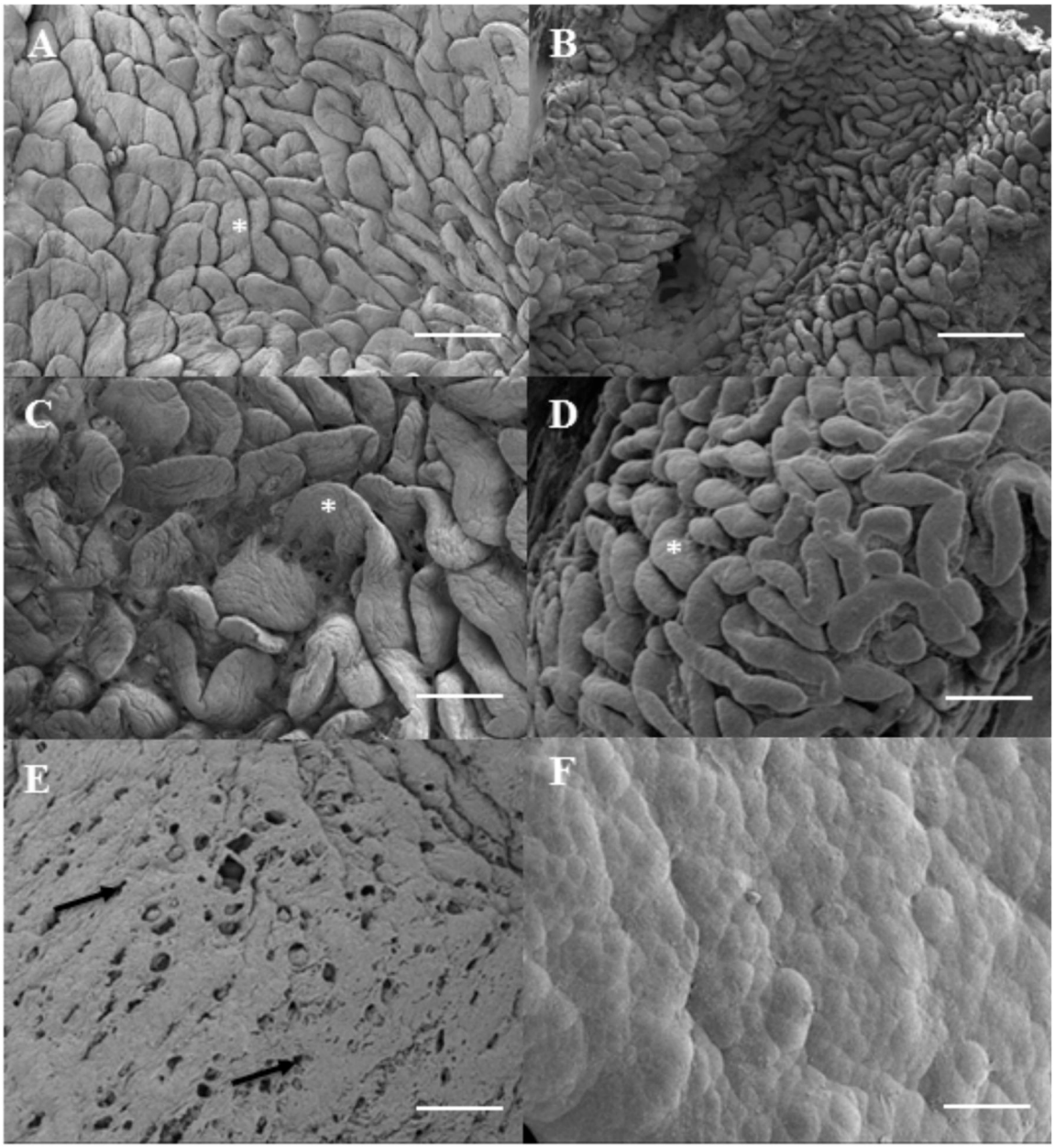


**Figure 4.**

Topography of native intestinal tissue, including complex villus structures (A,C), is mimicked in vapor deposited positive Parylene molds (B,D). Top view shown, *denote villus structures, black arrow denotes pores. Bar = 1mm in (A,B) and 500 μM in (C,D).

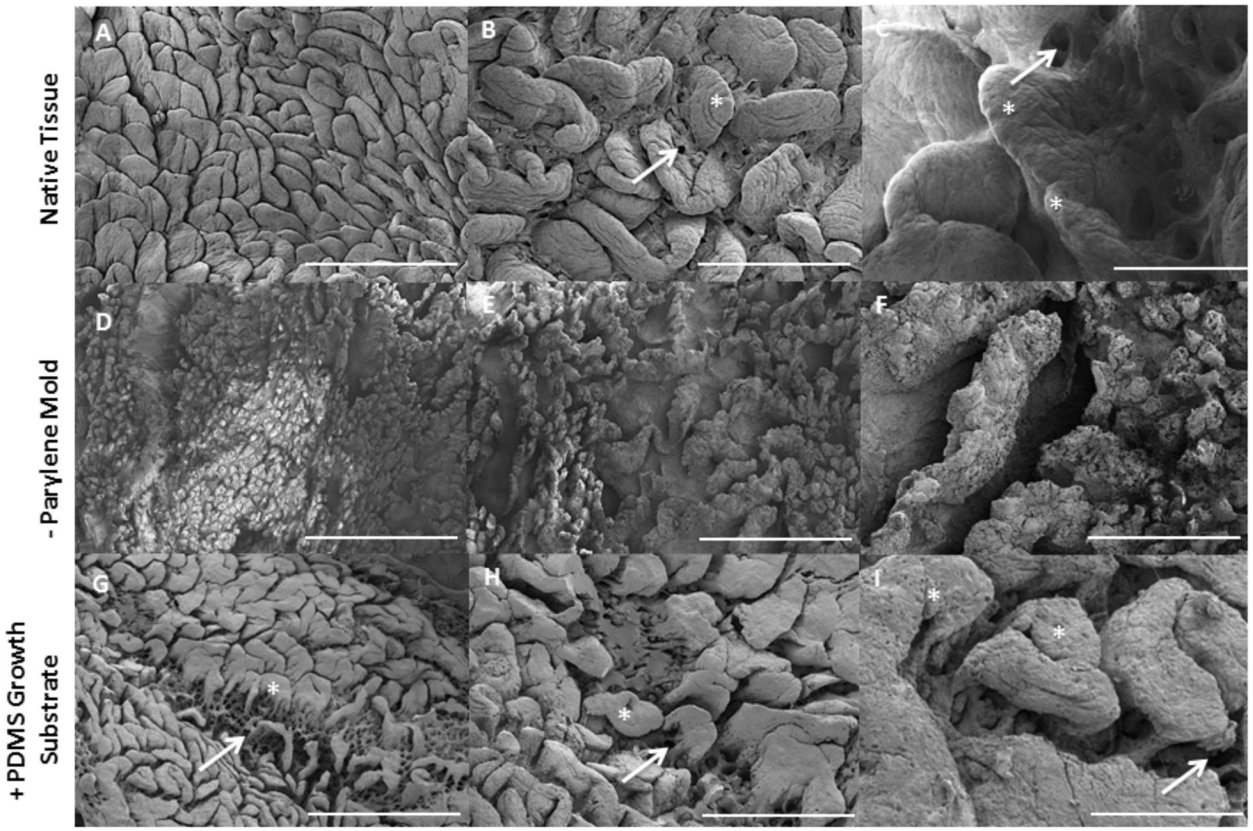


**Figure 5.**

Small intestinal multi-scale features shown on native tissue (A–C) are imprinted into negative Parylene molds (D–F) used for solution casting of positive PDMS replicas (G–I) as biomimetic growth substrates. A,D,G bar = 1 mm; B,E,H bar = 500 μM; C,F,I bar = 200 μM, * denotes villus structure, arrow denotes crypt.

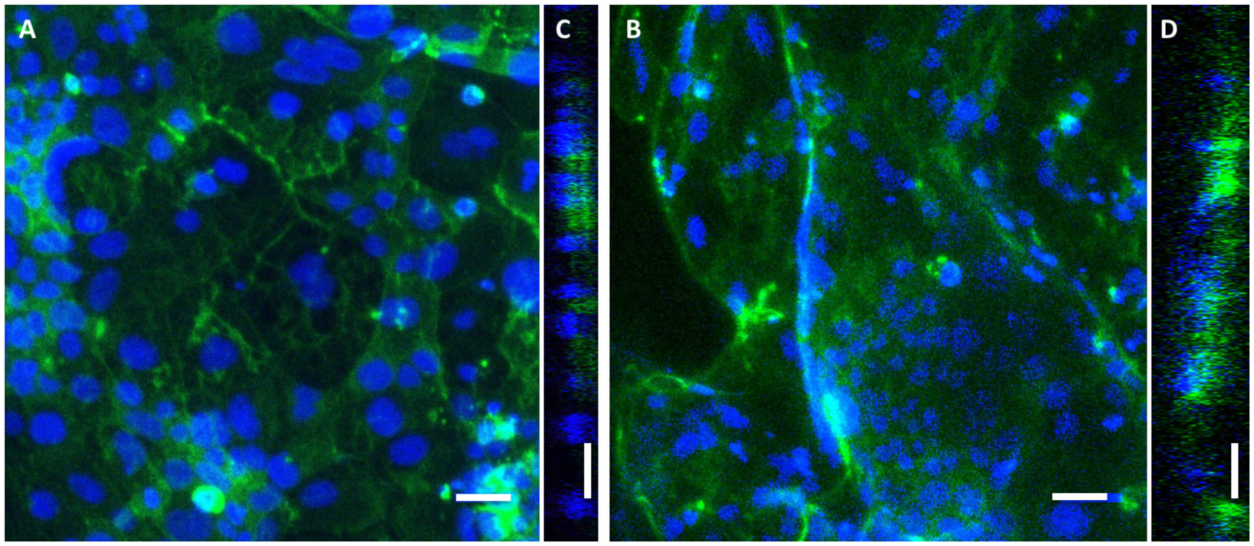


**Figure 6.**

Representative fluorescent images of Caco-2 monolayers cultured for 10 days on flat PDMS substrates (a) and biomimetic PDMS replicas (b). Optical cross sections of growth substrates are shown as Y-orthogonal views of the flat (c) and replica (d) substrate surfaces. Blue = Hoechst nuclei, green = filamentous actin cytoskeleton. Bars = 50 um. Confocal maximum intensity projections shown.

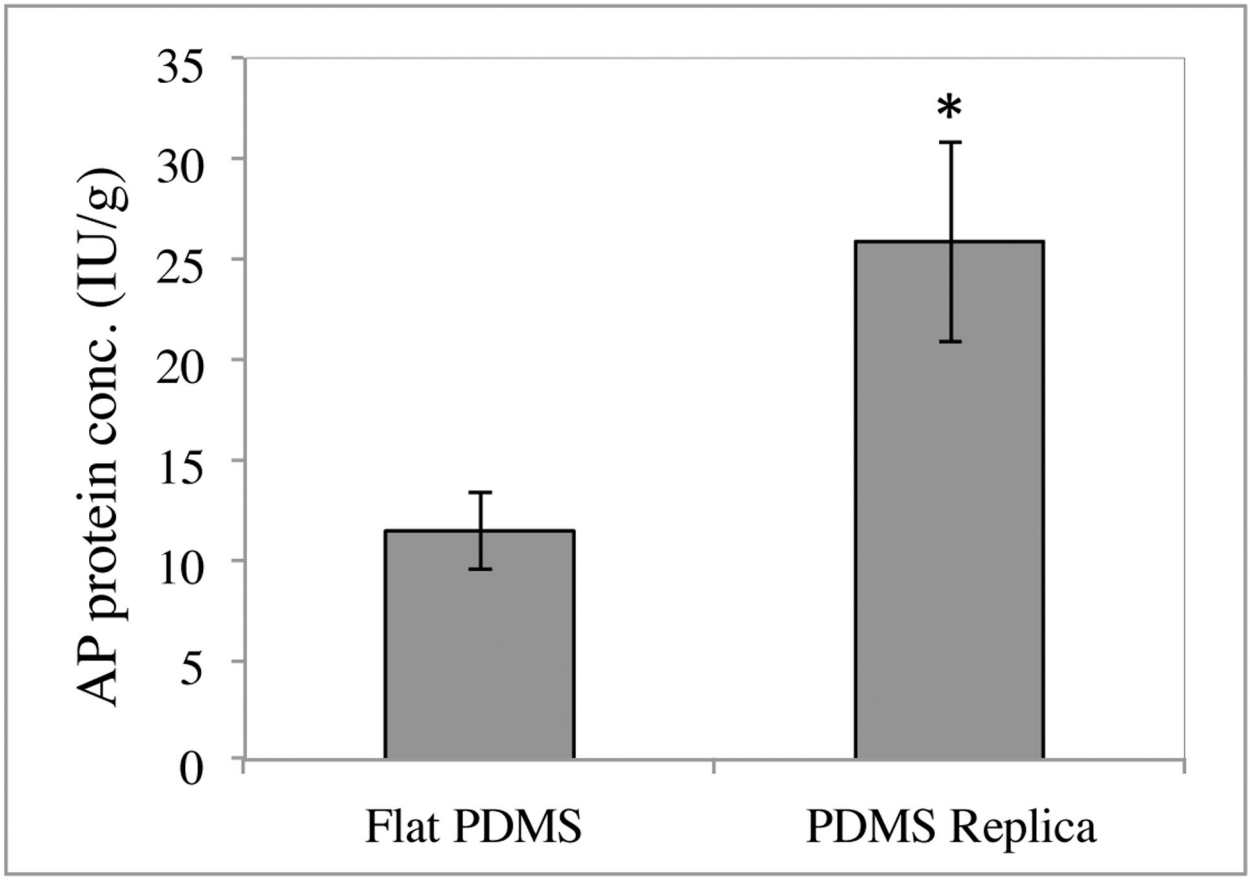


**Figure 7.**

Alkaline phosphatase (ALP) expression of Caco-2 cells is enhanced on topographical replicas of native small intestine (right) compared to flat controls (left). Cells were cultured for 10 days prior to measuring ALP, n = 3, * = $p < 0.05$